Nonlinear reactive systems on a lattice viewed as Boolean dynamical systems

E. Abad,* P. Grosfils, and G. Nicolis
Centre for Nonlinear Phenomena and Complex Systems, Université Libre de Bruxelles, Campus Plaine, Code Postal 231, B-1050 Bruxelles, Belgium

(Received 22 August 2000; published 19 March 2001)

We present a stochastic, time-discrete Boolean model that mimics the mesoscopic dynamics of the desorption reactions $A+A\rightarrow A+S$ and $A+A\rightarrow S+S$ in a one-dimensional lattice. In the continuous-time limit, we derive a hierarchy of dynamical equations for the subset of moments involving contiguous lattice sites. The solution of the hierarchy allows to compute the exact dynamics of the mean coverage for both microscopic and coarse-grained initial conditions, which turn out to be different from the mean field predictions. The evolution equations for the mean coverage and the second-order moments are shown to be equivalent to those provided by a time-continuous master equation. The important role of higher-order fluctuations is brought out by the failure of a truncation scheme retaining only two-particle fluctuation correlations.

DOI: 10.1103/PhysRevE.63.041102 PACS number(s): 05.40.−a, 05.45.−a

I. INTRODUCTION

When reactive processes take place in low-dimensional spaces, the mean-field (MF) laws of classical kinetics, in which each particle is assumed to interact with the system as a whole, become questionable. In this simple one-particle picture, information about special geometric constraints or many-particle correlation effects is absent. However, these features become increasingly important as the dimensionality of the space decreases and may eventually give rise to a crossover between universal macroscopic MF behavior and specific, strongly lattice-dependent behavior below a critical dimension d_c. The critical dimension d_c is found to depend on the characteristics of the support (such as average coordination number) and the stoichiometry of the reactive dynamics, i.e., its degree of nonlinearity.

The crossover phenomenon mentioned above is not specific to reactive systems, but is common to many other statistical systems (interacting spins, random walks, etc.). To understand its real nature, it is necessary to resort to a more refined description in which relevant fluctuation effects in concentration and occupation number space can be accounted for. In view of the difficulties encountered by a full-scale microscopic analysis, one typically tries to devise ''minimal'' models that contain the necessary ingredients to observe a significant departure of MF behavior at sufficiently low dimensions. A probabilistic, time-continuous approach of this kind for a detailed study of fluctuations is provided by master equation (ME) techniques in which the local dynamics is specified by transition rates between different microscopic states. In the ME approach, one is typically led to a set of evolution equations for the moments of the probability density, which can be taken as a starting point to compute the most characteristic macroscopic observables, generally associated with the first low-order moments. However, if the transition rates are nonlinear, the low-order moments will not obey closed equations but will rather be linked to the higher-order ones by an infinite hierarchy of coupled equations. In the general case, these hierarchies cannot be solved in a closed form. Suitable truncation techniques may then help to overcome this difficulty.

A more recent, very successful method of studying the evolution of low-dimensional reactive systems is based on Monte Carlo (MC) simulations [1], in which the microscopic state of the system is updated at discrete time steps according to a given dynamical rule. One of our goals in this paper is to establish a link between the physics underlying this simulational approach and the ME formalism. To this end, we shall formulate mathematically the evolution law prescribed by the MC algorithm as a stochastic dynamical system whose state variables are Boolean occupation numbers for the state of each lattice site [2,3]. As we shall see, this cellular automaton (CA) model yields a set of moment equations similar to that obtained from a time-continuous ME.

So far, most of the literature devoted to the effects of dimensionality on reactive dynamics has focused on diffusion-controlled reactions [4–6]. In these systems, deviations of MF behavior at low dimensions may be expected due to the reduced effective mobility of the reactants. There are, however, situations in which diffusion can be neglected within the time scale of interest, like, e.g., chemical reactions in solid materials and certain radical isolation problems [7]. Such systems of immobile reactants constitute the object of our study in this paper. Clearly, the absence of diffusion reduces the ability of each particle to interact with all the others, thus driving the system further away from the applicability conditions of MF theory. This effect is enhanced in the presence of short-range interactions restricted to, say, nearest neighbors and hard core exclusion not allowing more than one particle per lattice site [8–12].

More specifically, we will study the one-dimensional (1D) lattice dynamics in two particular examples of nonlinear irreversible reactions associated with the cooperative desorption systems (CDs)

$$A+A\xrightarrow{k_R}A+S, \quad \text{cooperative partial desorption (CPD)} \tag{1a}$$

*Email address: eabad@ulb.ac.be

$$A+A \xrightarrow{k_R} S+S, \quad \text{cooperative total desorption (CTD)}, \tag{1b}$$

where A is the reactive species, S the empty lattice site, and k_R is the rate of reaction. Notice that steps (1a) and (1b) are typical parts of realistic, more complex reaction schemes as discussed further in the concluding section. Despite their apparent simplicity, they display a complex non-MF behavior characterized by frozen, nonuniversal, initial-condition-dependent steady states [10,13,14]. The dependence on the initial conditions is the signature of the weak ergodic properties of the CDs, which is in turn related to the irreversibility of the reactive schemes (1a) and (1b). A remarkable feature of the CDs is the special structure of the underlying moment equations, which allows one to compute explicitly the coverage and the fluctuation dynamics and thus test in a very efficient way the applicability of diverse truncation approaches.

The paper is organized as follows. In Sec. II, a comprehensive study of the one-dimensional CPD is presented. First, we introduce a particular biased implementation of the CPD and characterize its non-MF behavior using an intuitive argument. In Sec. II B, we introduce a stochastic dynamical rule that mimics the microscopic, time-discrete evolution of the system as prescribed by MC simulations and show that this dynamical rule characterizes properly the steady states of the system. In Sec. II C, we derive evolution equations for the first- and second-order moments of the probability distribution for the microscopic states and use the same formalism to obtain a hierarchy of coupled equations describing the time evolution of a particular subset of moments, namely, those involving contiguous occupation numbers. These moments can be identified with the probabilities of finding a randomly chosen string of contiguous sites simultaneously occupied. In Sec. II D, it is found that the solution of the hierarchy for both microscopic and coarse-grained initial conditions leads to an explicit expression for the mean coverage of the lattice. We also derive equations for the coarse-grained dynamics of vacant sites in terms of generalized probabilities for occupied sites. Next, in Sec. II E, we present a general ME for an array of Boolean variables and show that in the special case of the CPD, the evolution equations for the mean occupation number and the second-order moment are similar to those obtained in the CA approach. In Sec. III, we study the relevance of inhomogeneous fluctuations in the CPD system. A set of evolution equations retaining only pair fluctuation correlations fails to reproduce the correct dynamics, the reason being the non-negligibility of higher-order fluctuation correlations. These can be calculated explicitly from sets of generalized moment equations, which also allow us to compute the dynamics of the vacant sites for clusters of small size. In Sec. IV, we extend the main results of Secs. II and III to the CTD. The conclusions are summarized in Sec. V, which also outlines a research strategy for future work in this area. In the Appendixes, we deal with a symmetric version of the CPD and discuss its equivalence with the biased CPD. We also study the dynamics of particle islands.

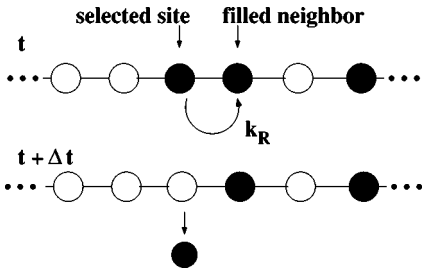

FIG. 1. Reaction step for the CPD. If the chosen site and a randomly chosen neighbor are filled, the reaction proceeds with rate k_R.

II. BOOLEAN DYNAMICS OF THE CPD: MODEL AND EXACT RESULTS

A. Definition of the system and MF rate equation

Consider a 1D lattice with N sites that may be either empty (S) or filled with a single particle (A). The reaction takes place according to the scheme of Fig. 1. At each time step Δt, a lattice site is randomly chosen. If the selected site is filled, the particle desorbs with a certain probability (equal to the rate of reaction k_R) provided that its right-neighbor site is also occupied; otherwise, nothing occurs. The classical rate equation for this CPD scheme [Eq. (1a)] reads

$$\frac{dc(t)}{dt} = -k_R c(t)^2, \tag{2}$$

where $c(t)$ is the A-particle concentration, here identified as the mean fraction of occupied sites, also referred to as ''coverage.'' Its solution predicts a decay of the form

$$c(t) = \frac{c(0)}{1+c(0)k_R t} \tag{3}$$

to a zero-coverage steady state. However, as we see below, the restricted 1D geometry of the lattice allows for non-MF steady states. It is indeed easily seen that all lattice configurations without contiguous particles cannot evolve in time. To understand this obvious MF failure in detail, we need to set up a model for the microscopic dynamics.

B. Boolean modeling and steady states

We stipulate that each site in the lattice is characterized by a Boolean occupation number

$$n_i(t) = \begin{cases} 1 & \text{if site i is occupied} \\ 0 & \text{if site i is empty,} \end{cases} \tag{4}$$

$i=1, \ldots, N$. Each site evolves according to the nonlinear dynamical rule

$$n_i(t+\Delta t) = n_i(t) - \xi_N^{(i)}(t)\xi_R(t)n_i(t)n_{i+1}(t), \quad i=1, \ldots, N, \tag{5}$$

where

$$\vec{\xi}_N(t)=\begin{pmatrix}\xi_N^{(1)}(t)\\ \vdots \\ \xi_N^{(N)}(t)\end{pmatrix}, \quad \xi_N^{(i)}(t)=0,1 \tag{6}$$

is a N-dimensional vector of stochastic Boolean decision variables. If, say, site i is chosen, the ith component will be one and all the other components will be zero. Hence, the different components $\xi_N^{(i)}(t)$ in a given, single realization are correlated:

$$\sum_{i=1}^{N}\xi_N^{(i)}(t)=1, \quad \xi_N^{(i)}(t)\xi_N^{(j)}(t)=\xi_N^{(i)}(t)\,\delta_{ij}. \tag{7}$$

Since at each time step Δt, one site out of N is randomly chosen, the mean value $\overline{\xi_N^{(i)}(t)}$ over an ensemble of realizations will be $1/N$. The additional stochastic variable $\xi_R(t)$ takes randomly the values 1 and 0 with probabilities p_R and $1-p_R$, respectively.

To have a well posed problem, we still have to specify the boundary conditions. We shall take periodic boundary conditions, which amount to setting $n_{N+1}(t)=n_1(t)$ in the last Eq. (5).

Implicit in the above scheme is the idea that, at most, one reactive event may occur in the lattice in a given time interval Δt, even if there are several *a priori* reactive pairs. The justification of such a prescription is that, typically, the occurrence of a reaction requires to overcome an activation energy threshold. At ordinary temperatures (supposed to prevail here), this can be achieved only if a sufficiently strong fluctuation impinges on the system as a result, say, of the coupling between the adsorbate and the lattice. Since the probability of such an event is small, one may expect that reactions will occur asynchronously at different lattice sites, which is precisely what is stipulated in our evolution rule.

Equations (5) will be used in the sequel to describe the dynamics of the CPD at three different levels.

(1) A ''microscopic'' level in which the exact microscopic dynamics, i.e., the initial condition $\{n_i(0)\}$ and the decision path represented by the variable sets $\{\vec{\xi}_N(0),\ldots,\vec{\xi}_N(t)\}$ and $\{\xi_R(0),\ldots,\xi_R(t)\}$, is assumed to be known in detail.

(2) An intermediate level in which the system is prepared in such a way that the initial condition is known in detail and one averages only over the subsequent dynamics, i.e. , over the different paths or realizations.

(3) A ''coarse-grained'' description in which one averages over a statistical ensemble of realizations *and* a nonequilibrium ensemble of initial conditions.

After a time t_{st} a steady state $\{n_i^{st}\}$ is attained. The dynamical rule (5) allows a straightforward characterization of these steady states. Since the first term in the right-hand side (rhs) of Eq. (5) cancels with the lhs, one has

$$\xi_N^{(i)}(t)n_i^{st}n_{i+1}^{st}=0. \tag{8}$$

This holds for all times $t\geqslant t_{st}$. Since $\xi_N^{(i)}(t)$ is a random variable, it will be nonzero at some time t for any given site i meaning that the product $n_i^{st}n_{i+1}^{st}$ must vanish for all i. This expresses the fact that two contiguous sites cannot be simultaneously occupied in a steady state. However, not all configurations satisfying this condition are attained with equal probability. For instance, if N is even, we can be certain that the steady-state configuration with alternating occupied and empty sites will never be reached if we start with less than half the lattice filled. Therefore, a simple combinatorial counting of the nonevolving configurations fails to provide the correct mean steady-state coverage [14].

C. Moment equations and cluster dynamics

Let us now turn to the dynamics generated by Eq. (5). First, we fix the initial configuration $(n_1(0),\ldots,n_N(0))$ of the lattice and take the average of Eq. (5) over an ensemble of different realizations. Using the statistical independence of $\overline{\xi_N(t)}$, $\xi_R(t)$, and the occupation numbers $n_i(t)$, this yields

$$\overline{n_i(t+\Delta t)}-\overline{n_i(t)}=-\frac{p_R}{N}\overline{n_i(t)n_{i+1}(t)}, \quad i=1,\ldots,N. \tag{9}$$

The quantity p_R/N can be regarded as the probability that a reaction takes place at a given site i in the time interval $(t,t+\Delta t)$ given that sites i and $i+1$ are occupied. The rate of reaction is obtained by dividing this probability by the time step Δt:

$$k_R=\frac{p_R}{N\Delta t}. \tag{10}$$

To derive the continuous-time limit of Eq. (9), we divide both sides by Δt and let this quantity go to zero in such a way that the reaction rate k_R remains finite. This can be, e.g., accomplished by letting the system size N simultaneously go to infinity so that $N\Delta t=C$. We shall choose the constant C equal to unity, implying that, after one time unit, each lattice site has been visited once on average. With this choice, k_R becomes numerically equal to the value of p_R. The resulting equation reads

$$\frac{d}{dt}\overline{n_i(t)}=-k_R\overline{n_i(t)n_{i+1}(t)}. \tag{11}$$

In a similar way, one can obtain an evolution equation for the second-order moment $\overline{n_i(t)n_j(t)}$. Multiplying Eq. (5) by $n_j(t+\Delta t)$ and using Eq. (7), one finds

$$\overline{n_i(t+\Delta t)n_j(t+\Delta t)}-\overline{n_i(t)n_j(t)}$$
$$=-\frac{p_R}{N}\overline{n_i(t)n_{i+1}(t)n_j(t)}-\frac{p_R}{N}\overline{n_i(t)n_j(t)n_{j+1}(t)}, \quad i\neq j, \tag{12}$$

which in the continuous-time limit becomes

$$\frac{d}{dt}\overline{n_i(t)n_j(t)} = -k_R\overline{n_i(t)n_{i+1}(t)n_j(t)} - k_R\overline{n_i(t)n_j(t)n_{j+1}(t)}. \tag{13}$$

For $j=i+1$, Eq. (13) together with the Boolean property $n_i^2(t)=n_i(t)$ yields

$$\frac{d}{dt}\overline{n_i(t)n_{i+1}(t)} = -k_R\overline{n_i(t)n_{i+1}(t)} - k_R\overline{n_i(t)n_{i+1}(t)n_{i+2}(t)}. \tag{14}$$

Unless otherwise specified, we shall set $p_R=1$ for simplicity, implying that k_R is equal to unity. Note, however, that it is possible to absorb the reaction rate k_R appearing in the time-continuous equations (11) and (13) in the time scale by means of a dimensionless variable $\tau=k_Rt$ [10,14].

An important feature of Eqs. (11) and (14) is that they couple in a linear fashion moments involving only contiguous sites. This turns out to be a generic property that also holds for the dynamics of higher-order moments.

Let us now consider a more general subset of k contiguous lattice sites $i,\ldots,i+k-1$. The probability of finding all sites occupied at time t, i.e., a cluster of size k, is given by the quantity

$$M_k^{(i)}(t) = \overline{\prod_{j=i}^{i+k-1} n_j(t)}, \quad i,k=1,\ldots,N. \tag{15}$$

To derive an evolution equation for $M_k^{(i)}(t)$, we must generalize Eqs. (11) and (14). Taking the dynamical rule (5) as a starting point, one obtains

$$\begin{aligned}\prod_{j=i}^{i+k-1} n_j(t+\Delta t) - \prod_{j=i}^{i+k-1} n_j(t) &= -\sum_{j=i}^{i+k-2} \xi_N^{(j)}(t)\xi_R(t) \prod_{j=i}^{i+k-1} n_j(t) \\ &\quad - \xi_N^{(i+k-1)}(t)\xi_R(t)\prod_{j=i}^{i+k} n_j(t),\end{aligned} \tag{16}$$

where $i=1,\ldots,N$. Taking averages in Eq. (16) for $k<N$, one gets

$$M_k^{(i)}(t+\Delta t) - M_k^{(i)}(t) = -\frac{(k-1)}{N}M_k^{(i)}(t) - \frac{1}{N}M_{k+1}^{(i)}(t). \tag{17}$$

We now introduce the global quantity

$$\overline{P}_k^{(N)}(t) = \frac{1}{N}\sum_{i=1}^{N} M_k^{(i)}(t), \tag{18}$$

representing the probability of finding k-filled adjacent sites in the N-site lattice. Summing over the site index i in Eq. (17), we find

$$\overline{P}_k^{(N)}(t+\Delta t) - \overline{P}_k^{(N)}(t) = -\frac{(k-1)}{N}\overline{P}_k^{(N)}(t) - \frac{1}{N}\overline{P}_{k+1}^{(N)}(t), \quad k<N. \tag{19}$$

Taking the continuous-time limit of Eq. (19) for a given finite value of k, a set of evolution equations for $\overline{P}_k(t) = \lim_{N\to\infty}\overline{P}_k^{(N)}(t)$ is obtained:

$$\frac{d\overline{P}_k(t)}{dt} = -(k-1)\overline{P}_k(t) - \overline{P}_{k+1}(t), \quad k=1,2,\ldots,k_{max}, \tag{20}$$

where the integer k_{max} is the size of the largest cluster. The first term on the rhs of Eq. (20) corresponds to a destruction of a k-particle cluster by the interaction of two particles inside the cluster, while the second term stands for its destruction by desorption of its rightmost particle, which requires an additional occupied site, i.e., a cluster of $k+1$ sites.

If the lattice contains only clusters of finite size, then $k_{max}<\infty$ and the hierarchy of Eq. (20) is truncated by the condition $\overline{P}_{k_{max}+1}(t)\equiv 0$. The last Eq. (20) reads then

$$\frac{d\overline{P}_{k_{max}}(t)}{dt} = -(k_{max}-1)\overline{P}_{k_{max}}(t). \tag{21}$$

D. Solution of hierarchy and mean coverage for microscopic and for coarse-grained initial conditions

Suppose that we start with a given initial configuration $\{n_i(0)\}$ characterized by the nonvanishing set of probabilities

$$\{\overline{P}_1(0),\overline{P}_2(0),\ldots,\overline{P}_{k_{max}}(0)\}. \tag{22}$$

Using the linearity of Eq. (20), one can show that the solution for $t>0$ is of the form

$$\overline{P}_k(t) = \exp\{-(k-1)t\}\sum_{j=0}^{k_{max}-k}\frac{\{\exp(-t)-1\}^j}{j!}\overline{P}_{k+j}(0), \quad k=1,\ldots,k_{max}. \tag{23}$$

Note that for $t\to\infty$ only $\overline{P}_1$ survives, representing the probability that a randomly chosen site be occupied. Clearly, this probability is equal to the ratio between the average number of occupied sites and the total number of sites, i.e., the mean coverage of the lattice $c(t)$. In the long-time limit, one has

$$c(\infty) = \overline{P}_1(\infty) = \lim_{N\to\infty}\frac{\overline{N_A(\infty)}}{N} = \sum_{j=0}^{k_{max}-1}\frac{(-1)^j}{j!}\overline{P}_{j+1}(0). \tag{24}$$

We see that the asymptotic value of the coverage depends on all details of the initial cluster distribution. The validity of Eq. (24) is confirmed by MC simulations [Fig. 2(a)]. The simulations were performed according to the time-discrete rule (5). The data correspond to a chain ring of 100 particles and the initial configurations

$$C1 = 11111111111111101111111111101111011111111111111101111111111111111$$
$$11101111111011011111111011111010,$$

$$C2 = 01111001111110010011110111110111011111111110100011111111011011001111$$
$$11011101001111101011111111101111,$$

$$C3 = 11010101101001100100101010010010000101001011101001001001011001001111$$
$$01100011111001011001101001100111,$$

$$C4 = 10011100111000010011011000001000000000001000010010010010011000101000$$
$$01001010010101000011001101100010.$$

Let us now assume the more realistic situation in which the initial configuration of the system is not known in detail, but is characterized only through the particle coverage p. If we consider a uniform ensemble of all random microscopic configurations with a given p, the system will initially be translationally invariant and this property will propagate in time. Thus, the probabilities of finding k consecutive filled sites $i, \ldots, i+k-1$

$$P_k^{(N)}(t) = \left\langle \prod_{j=i}^{i+k-1} n_j(t) \right\rangle, \quad k = 1, \ldots, N \tag{25}$$

(the angular brackets $\langle \cdots \rangle$ stand for the averaging over realizations *and* initial states) will not depend on the evaluation site i. After averaging Eq. (17) over the initial conditions and going over to the time continuum, one obtains

$$\frac{dP_k(t)}{dt} = -(k-1)P_k(t) - P_{k+1}(t) \quad k = 1,2, \ldots, \tag{26}$$

which is formally identical to Eq. (20) for $\overline{P_k}$ with $k_{max} \to \infty$. However, the initial conditions are now simpler. Since the initial occupancies of each site are statistically independent, one has

$$P_k(0) = p^k, \quad k = 1,2, \ldots . \tag{27}$$

A solution satisfying the initial conditions (27) can be easily found by using an ansatz suggested in [10]. One obtains

$$P_1(t) = p \exp[p\{\exp(-t) - 1\}], \tag{28a}$$

$$P_k(t) = p^{k-1} \exp[-(k-1)t] P_1(t), \quad k = 2,3, \ldots . \tag{28b}$$

Again, the survival expectancy $P_1(t)$ corresponds to the mean coarse-grained coverage $c(t) = \lim_{N \to \infty} \langle N_A(t) \rangle / N$. For short times, the series expansion of Eq. (28a) yields

$$c(t) = P_1(t) = p - p^2 t + \frac{p^2(p+1)}{2} t^2 + o(t^3). \tag{29}$$

It is interesting to compare this with the short-time behavior of the exact solution of the MF equation (2). Setting $K_R = 1$ for simplicity, one has

$$c_{MF}(t) = \frac{p}{1+pt} = p - p^2 t + p^3 t^2 + o(t^3). \tag{30}$$

Thus, we see that the first MF deviation appears in the second-order term. For long times, one observes an exponential decay into an absorbing state characterized by the asymptotic coverage

$$c(\infty) = p \exp(-p). \tag{31}$$

Formulas (28) for the transient behavior and formula (31) for the asymptotics are confirmed by time-discrete MC simulations [Fig. 2(b)]. As in the previous case, all $P_k(t)$ with $k \geqslant 2$ vanish for $t \to \infty$. Note that Eqs. (28) are formally obtained from Eqs. (23) by averaging over a uniform distribution of microscopic states with global coverage p. This amounts to allowing for clusters of arbitrarily large size, i.e., $k_{max} \to \infty$.

So far, we have only considered the dynamics of particles, but it is also of interest to ask for the time evolution of empty intervals of a given size inside the lattice. Clearly, the number of empty intervals must grow as the reactions proceed. To set up explicit equations for clusters of vacant sites (''holes''), we consider the time-discrete evolution equation for the complementary occupation number $s_i(t) = 1 - n_i(t)$,

$$s_i(t+\Delta t) - s_i(t) = \xi_N^{(i)} n_i(t) n_{i+1}(t), \quad i = 1, \ldots, N. \tag{32}$$

By averaging this equation over an ensemble of realizations and a uniform initial distribution of microscopic states with a coverage p one gets

$$\frac{dS_1(t)}{dt} = P_2(t), \tag{33a}$$

where $S_1(t) = \langle s_i(t) \rangle$. Equation (33a) is in agreement with the conservation law $(d/dt)[P_1(t) + S_1(t)] = 0$.

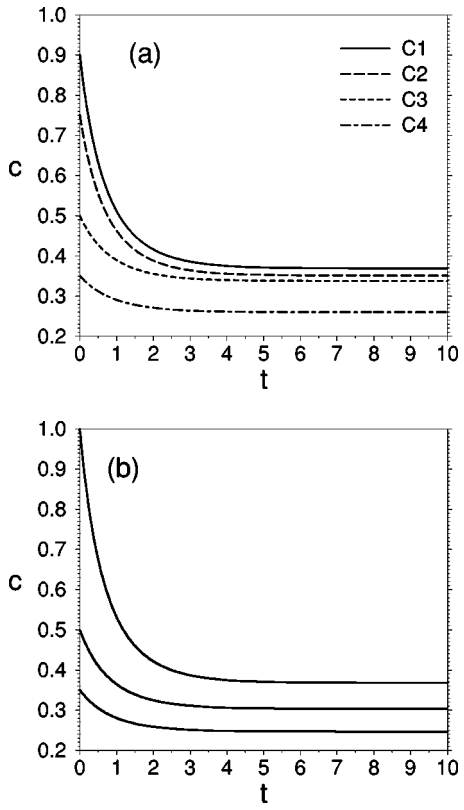

FIG. 2. (a) Mean coverage $c(t)=\overline{P}_1(t)$ for the four different initial configurations $C1-C4$ computed from MC simulations over 10^4 realizations. Both the dynamics and the asymptotic value of the coverage are in excellent agreement with formulas (23) and (24). The final saturation at different coverage values reflects the dependence on the initial conditions, and hence, the weak ergodic properties of the system. (b) Time evolution of the coarse-grained coverage $c(t)=P_1(t)$ computed from MC simulations over 10^2 realizations for a periodic lattice of 10^4 sites and $p=0.35,0.5$, and 1 (full lattice). As in (a), the final saturation value depends on the initial coverage p. Note, in addition, the monotonic dependence for all times of $c(t)$ as a function of the initial coverage p.

The dynamics of hole multimers can be derived starting from the evolution equation for the product $\Pi_{k=i}^{i+k-1}s_k(t)$. The general form of the evolution equation for $S_k(t)=\langle\Pi_{k=i}^{i+k-1}s_k(t)\rangle$ becomes more and more complicated with increasing cluster size. The next three equations read

$$\frac{dS_2(t)}{dt}=P_2(t)-P_3(t), \tag{33b}$$

$$\frac{dS_3(t)}{dt}=P_2(t)-P_3(t)+P_4(t)-P_{1,2}^{(2)}(t), \tag{33c}$$

$$\frac{dS_4(t)}{dt}=P_2(t)-P_3(t)+P_4(t)-P_5(t)-P_{1,2}^{(2)}(t)+P_{1,3}^{(2)}(t)+P_{2,2}^{(2)}(t)-P_{1,2}^{(3)}(t), \tag{33d}$$

where the quantities $P_{n,m}^{(l)}(t)$ on the rhs of Eqs. (33c) and (33d) are the joint probabilities of finding two fully occupied strings of length n and m separated by l lattice spacings. The initial conditions for which these equations must be solved are

$$S_k(0)=(1-p)^k, \quad k=1,2,\ldots. \tag{34}$$

Equations (33a) and (33b) can be integrated straightforwardly, since the functions on the rhs are already explicitly known. In Sec. III, we show how to obtain explicit expressions for the probabilities $S_3(t)$ and $S_4(t)$ by solving a generalized hierarchy for the joint probabilities $P_{n,m}^{(l)}(t)$.

E. Comparison with the ME approach

An alternative way of deriving moment equations in the framework of a time-continuous approach is provided by the master equation (ME). Let us again consider a set of N Boolean variables $\{n\}=(n_1,\ldots,n_N)$ arranged on the sites of a 1D lattice with periodic boundaries ($n_{N+1}=n_1$). Starting from an arbitrary state, the evolution of the probability density $P(\{n\};t)$ is governed by a ME of the form

$$\frac{dP(\{n\};t)}{dt}=-\sum_j w_j(\{n\}\to\{n'\},t)P(\{n\};t)+\sum_j w_j(\{n'\}\to\{n\},t)P(\{n'\};t), \tag{35}$$

where $\{n'\}=(n_1,\ldots,1-n_j,\ldots,n_N)$ and $w_j(\{n\}\to\{n'\},t)$ is the transition rate from the state $\{n\}$ to the state $\{n'\}$ at time t. To obtain an evolution equation for the average occupation number

$$\langle n_i(t)\rangle=\sum_{\{n\}} n_i(t)P(\{n\},t), \tag{36}$$

we multiply Eq. (35) by $n_i(t)$ and sum over all different configurations $\{n\}$. This yields

$$\frac{d}{dt}\langle n_i(t)\rangle=\langle[1-2n_i(t)]w_i(\{n\}\to\{n'\},t)\rangle. \tag{37}$$

For the time evolution of the second-order moment, one gets

$$\frac{d}{dt}\langle n_i(t)n_j(t)\rangle=\langle[n_j(t)-2n_i(t)n_j(t)]w_i(\{n\}\to\{n'\},t)\rangle+\langle[n_i(t)-2n_i(t)n_j(t)]w_j(\{n\}\to\{n'\},t)\rangle, \quad i\neq j. \tag{38}$$

For the CPD, the transition rate reads

$$w_j(\{n\}\to\{n'\},t)=k_R n_j(t)n_{j+1}(t). \tag{39}$$

Using Eqs. (37) and (38) and the transition probability (39) with $k_R=1$, one can formally recover Eqs. (11) and (13) averaged over an ensemble of random initial conditions. As expected, this also holds for the higher order moments [14]. Note that in the ME approach the double averaging over realizations and initial conditions is performed *simultaneously* via the probability distribution $P(\{n\},t)$. In the CA

model, this has been done in two separate steps. One first chooses randomly an initial condition with a given p and thereafter performs a series of different realizations. Next, one again selects a new random initial condition and a new set of realizations is carried out, and so on.

III. TRUNCATION SCHEMES AND THE ROLE OF FLUCTUATIONS IN THE CPD

The statistical properties of the N-site CPD system are described by the ''Boltzmann-like'' distribution functions $c^{(N)}_{i_1,i_2\ldots,i_n}(t)=\langle n_{i_1}(t)n_{i_2}(t),\ldots,n_{i_n}(t)\rangle$, which can be expressed in terms of the mean occupations $c^{(N)}_i(t)=\langle n_i(t)\rangle$ and a set of correlation functions

$$f^{(N)}_{i_1 i_2,\ldots,i_n}(t_1;\ldots;t_n)=\langle \delta n_{i_1}(t_1)\,\delta n_{i_2}(t_2)\cdots\delta n_{i_n}(t_n)\rangle, \tag{40}$$

where $\delta n_i(t)=n_i(t)-c^{(N)}_i(t)$. In the following, we shall omit the superscript N in the quantities c and f for the sake of notational simplicity. For $n=2$ and $t_1=t_2=t$, Eq. (40) defines the equal-time pair correlation function $f_{i,j}(t)\equiv f_{i,j}(t;t)$.

An approximate closure to the hierarchy equations can be obtained by performing an expansion in terms of correlation functions and keeping them up to a certain order, neglecting the higher-order ones. In this so-called Ursell expansion one defines the correlation functions f through the relations

$$c_{i,j}(t)=c_i(t)c_j(t)+f_{i,j}(t), \tag{41a}$$

$$c_{i,j,k}(t)=c_i(t)c_j(t)c_k(t)+c_k(t)f_{i,j}(t)+c_i(t)f_{j,k}(t)+c_j(t)f_{i,k}(t)+f_{i,j,k}(t), \tag{41b}$$

etc., where the quantities $f_{i,j}$ and $f_{i,j,k}$ account for the fluctuations

$$f_{i,j}(t)=\langle \delta n_i(t)n_j(t)\rangle \tag{42a}$$

$$f_{i,j,k}(t)=\langle \delta n_i(t)\,\delta n_j(t)\,\delta n_k(t)\rangle, \tag{42b}$$

etc. Different approximations emerge from Eqs. (41) when terms containing correlation functions of higher orders are neglected.

In the zeroth approximation all correlations between occupation numbers are neglected and the state of the system is completely specified by the mean occupation numbers $c_i(t)$. From Eq. (9) we have the MF equation

$$c_i(t+\Delta t)=c_i(t)-\frac{1}{N}c_i(t)c_{i+1}(t). \tag{43}$$

In the first approximation the rate equation (43) is extended with a term linear in the NN pair correlation $f_{i,i+1}(t)$,

$$c_i(t+\Delta t)=c_i(t)-\frac{1}{N}c_i(t)c_{i+1}(t)+\frac{1}{N}f_{i,i+1}(t). \tag{44}$$

Equation (44) describes the corrections to the MF equation (43) caused by the fluctuations $f_{i,i+1}(t)$ that are built up by sequences of correlated reactions between the particles. These correlations are calculated from the second hierarchy equation (12) with $j=i+1$. Neglecting terms in $O(1/N^2)$ and higher in the rhs, we have

$$\begin{aligned} f_{i,i+1}(t+\Delta t)=&-\frac{1}{N}c_{i+1}(t)f_{i,i+2}(t)+f_{i,i+1}(t)\\ &-\frac{1}{N}\{c_i(t)c_{i+1}(t)-c_i(t)[c_{i+1}(t)]^2\\ &+c_{i+2}(t)f_{i,i+1}(t)-c_{i+1}(t)f_{i,i+1}(t)\\ &+f_{i,i+1}(t)\} \end{aligned} \tag{45}$$

Here the first term in curly brackets represents the propagation to neighboring sites of fluctuations correlated over a distance of two lattice spacings. The other terms essentially contain the correlations created or destroyed by the reaction process; the terms linear in $f_{i,i+1}$ represent the effect of existing prereaction correlations, and the quantity

$$-\frac{1}{N}c_i(t)c_{i+1}(t)+\frac{1}{N}c_i(t)[c_{i+1}(t)]^2 \tag{46}$$

accounts for the correlations created by the reaction from a completely factorized state. The other pair correlations are calculated in a similar way from Eq. (12) with $j=i+l$

$$\begin{aligned} f_{i,i+l}(t+\Delta t)=&f_l(t)-\frac{1}{N}c_i(t)f_{i+1,i+l}(t)\\ &-\frac{1}{N}(c_{i+1}(t)+c_{i+l+1}(t))f_{i,i+l}(t)\\ &-\frac{1}{N}c_{i+l}(t)f_{i,i+l+1}(t)+O(1/N^2)\\ &+\text{higher-order terms},\quad l=2,\ldots,[N]/2. \end{aligned} \tag{47}$$

In the spatially homogeneous case, the system is translationally invariant; the solution obeys the relation $c_i(t)=c(t)$ and the correlations $f_{i,j}(t)=f_{|i-j|}(t)$ depend only on the relative distance between the evaluation sites. In the limit $N\to\infty$, Eqs. (44), (45) and (47) yield the following set of time-continuous equations:

$$\frac{dc(t)}{dt}=-c(t)^2-f_1(t), \tag{48a}$$

$$\frac{df_1(t)}{dt}=c(t)^2\{c(t)-1\}-f_1(t)-c(t)f_2(t), \tag{48b}$$

$$\frac{df_l(t)}{dt}=-c(t)[f_{l-1}(t)+2f_l(t)+f_{l+1}(t)],\quad l=2,3,\ldots. \tag{48c}$$

Equations (48) can be used as a starting point for a truncation based on the neglect of pair correlations $f_l(t)$ for all l equal

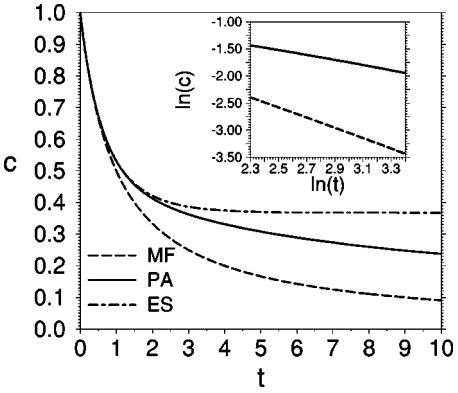

FIG. 3. Time evolution of the mean concentration $c(t)$ according to the rate equation (2) with $k_R=1$ (curve MF), the exact solution (28a) (curve ES), and the numerical solution for the pair approximation of the truncation hierarchy (48) (curve PA). Initially, the lattice is assumed to be fully occupied ($p=1$). In contrast to the exact solution, the truncated one decays slowly to the MF steady state. The inset shows a log-log plot of the concentration for long times for the MF and the truncated solution.

to or larger than a certain cutoff integer l_c. For $l_c=2$, i.e., in the pair approximation, the system of two equations approaches the steady state (0,0), although the asymptotic decay of $c(t)$ is much slower than the t^{-1} decay prescribed by the MF approach due to large transient effects in $f_1(t)$ (Fig. 3). A log-log plot of the numerical solution suggests an inverse power law behavior of $c(t)$ for long times with an exponent less than one (see inset in Fig. 3). In the pair approximation, the stability of the MF fixed point can be proven by geometric arguments.[1] Numerical results suggest that this property holds for any arbitrary l_c, meaning that the system truncated to any order will always attain the MF steady state of zero concentration, in contradiction with the non-MF results reported above. This reflects the non-negligibility of the three-point fluctuation correlations $f_{i,j,k}(t)$ which, as we shall see presently, indeed become of the same order of magnitude as the pair correlations $f_l(t)$ already for small l.

One can compute exactly these correlation fluctuations by considering the evolution equation for the joint probabilities $P^{(l)}_{j,k}(t)$, which in our model correspond to the distribution functions

$$\left\langle \prod_{r=i}^{i+j-1} n_r(t) \prod_{s=i+j+l-1}^{i+j+l+k-2} n_s(t) \right\rangle. \tag{49}$$

Taking Eq. (16) as a starting point, a tedious but straightforward calculation shows that $P^{(l)}_{j,k}(t)$ evolves according to

$$\frac{dP^{(l)}_{j,k}(t)}{dt} = -(j-1)P^{(l)}_{j,k}(t) - (k-1)P^{(l)}_{j,k}(t) - P^{(l-1)}_{j+1,k}(t) - P^{(l)}_{j,k+1}(t), \quad j,k,l=1,2,\ldots. \tag{50}$$

[1]This is illustrated by an analysis of the 2D velocity field.

The first (second) term on the rhs of Eq. (50) corresponds to an event in which a particle inside the cluster of j (k)-occupied sites desorbs by interaction with a neighbor inside the cluster, while the third (fourth) term stands for the desorption of the rightmost particle inside the cluster by reaction with an occupied neighbor site at its right. Equation (50) is solved using the ansatz

$$P^{(l)}_{j,k}(t) = p^{j+k-2}\exp[-(j+k-2)t]P^{(l)}_{1,1}(t), \quad j,k=1,2,\ldots. \tag{51}$$

This leads to the (infinite) coupled set of equations

$$\frac{dP^{(l)}_{1,1}(t)}{dt} = -p\exp(-t)[P^{(l)}_{1,1}(t) + P^{(l-1)}_{1,1}(t)], \quad l=2,3,\ldots, \tag{52}$$

with the boundary condition $P^{(1)}_{1,1}(t)=P_2(t)$. An explicit expression for $P^{(l)}_{1,1}(t)$ can be obtained from Eq. (52) by means of a generating function [15]. The final result reads

$$P^{(l)}_{1,1}(t) = P_1(t)\left\{ p\sum_{k=0}^{l-1}\left[\ln\left(\frac{P_1(t)}{p}\right)\right]^k \Big/ k! + \left[\ln\left(\frac{P_1(t)}{p}\right)\right]^l /l! \right\}. \tag{53}$$

This allows to compute the fluctuation correlation $f_l(t)$, which is given by

$$f_l(t) = P^{(l)}_{1,1}(t) - [P_1(t)]^2, \quad l=1,2,\ldots. \tag{54}$$

This function decreases superexponentially with increasing distance l, approaching zero for $l\to\infty$. The three-point nearest neighbor (NN) fluctuation correlation $h(t) = \langle \delta n_i \delta n_{i+1} \delta n_{i+2}\rangle$ can be expressed as

$$h(t) = P_3(t) - [P_1(t)]^3 - \{2f_1(t) - f_2(t)\}P_1(t). \tag{55}$$

Formulas (54) and (55) are confirmed by numerical simulations (Fig. 4). These also show that $h(t)$ may already get larger than $f_l(t)$ for $l=2$. In fact, the asymptotic values $h(\infty)$ and $f_2(\infty)$ are of the same order of magnitude in the whole range of the initial coverage p (Fig. 5). Higher-order fluctuations become comparatively large in the dilute limit $p\ll 1$.

In the light of the above, the failure of the truncation scheme seems thus to be due to the fact that it includes pair correlations of arbitrary long range without taking relevant higher-order fluctuations into account from the very beginning. Although we have only shown the non-negligibility of correlations up to the third order, some numerical computations suggest that, regardless of the initial conditions chosen, it is necessary to take into account the whole set of fluctuation correlations to obtain a deviation from the MF steady state.

A more restrictive truncation scheme consists in neglecting the effect of large clusters in Eqs. (26) by setting

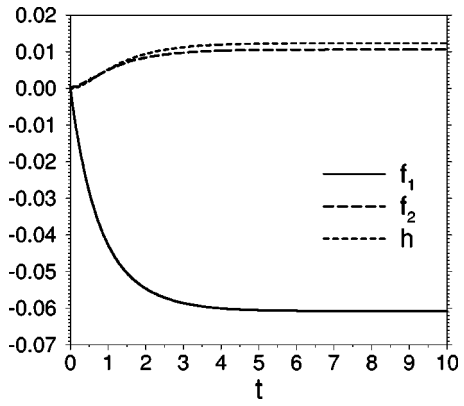

FIG. 4. Time evolution of $f_1(t), f_2(t)$, and $h(t)$ computed from MC-simulations over 10^2 realizations for a periodic lattice with $N=10^4$ and $p=0.35$. Asymptotically, $f_2(t)$ is nearly an order of magnitude smaller than $f_1(t)$, in accordance with the strong spatial decay predicted by formula (54). In contrast, the three-point correlation $h(t)$ is of the same order of magnitude as $f_2(t)$.

$P_k(t)\equiv 0$ beyond a given size [14]. This truncation procedure yields a smooth expansion of the exact results (28) and (31) in powers of p.

To conclude this section, let us note that the explicit knowledge of the joint probabilities $P^{(l)}_{j,k}(t)$ can be used to integrate Eqs. (33c) and (33d). The solutions of Eqs. (33) read

$$S_1(t)=1-P_1(t), \tag{56a}$$

$$S_2(t)=1-2P_1(t)+P_2(t), \tag{56b}$$

$$S_3(t)=1+(-3+p-\tfrac{1}{2}p^2)P_1(t)+2P_2(t)-\tfrac{1}{2}P_3(t), \tag{56c}$$

$$S_4(t)=1+(-4+3p-2p^2+\tfrac{1}{3}p^3)P_1(t)+(3-p+\tfrac{1}{2}p^2)\times P_2(t)-P_3(t)+\tfrac{1}{6}P_4(t). \tag{56d}$$

They are shown in Fig. 6 for the case of an initially full lattice.

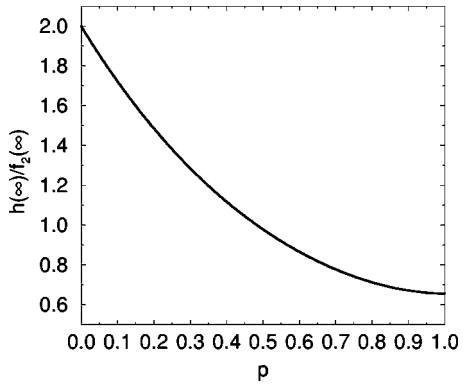

FIG. 5. p dependence of the asymptotic ratio $h(\infty)/f_2(\infty)$ computed from the formulas (54) and (55). For decreasing p, three-point fluctuations become increasingly important.

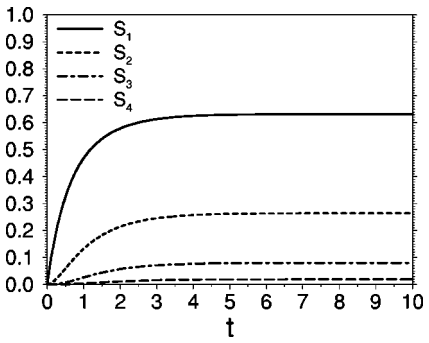

FIG. 6. Analytical solution of the first four evolution equations for intervals of vacant sites ($p=1$). The quantities S_1-S_4 grow monotonically due to the empty segments created by the reaction.

IV. DYNAMICS OF THE CTD

The starting point is again a 1D lattice with empty (S) and occupied sites (A). The reaction now proceeds according to the scheme depicted in Fig. 7. At each time step, one site is randomly chosen. If the chosen site and its neighbor are occupied, *both* particles will desorb with probability k_R. The classical rate equation reads

$$\frac{dc(t)}{dt}=-2k_Rc(t)^2, \tag{57}$$

which yields a faster decay than Eq. (2) to a zero-concentration steady state, but again proportional to t^{-1} for long times. It is easily seen that the actual 1D system has the same steady states as the CPD system, i.e. all configurations with isolated particles. Once more, a deviation from the MF behavior is found.

To set up the corresponding microscopic evolution law, we must take into account that this time a particle at a given site i will also desorb if its left-neighbor site $i-1$ is chosen and it is occupied. One has, therefore, an additional contribution in the rhs of the dynamical rule

$$n_i(t+\Delta t)=n_i(t)-\xi_N^{(i)}(t)\xi_R(t)n_i(t)n_{i+1}(t) -\xi_N^{(i-1)}(t)\xi_R(t)n_{i-1}(t)n_i(t), \quad i=1,\ldots,N. \tag{58}$$

As in the CPD case, we can take Eq. (58) as a starting point to derive evolution equations for the first- and the second-order moments

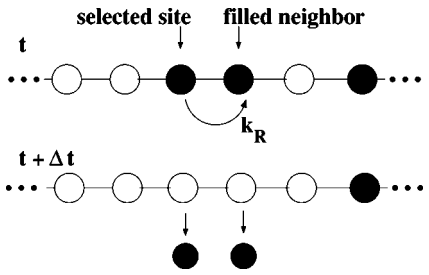

FIG. 7. Reaction step for the CTD. In contrast to the CPD case, both interacting particles desorb when the event takes place.

$$\frac{d}{dt}\overline{n_i(t)} = -\overline{n_{i-1}(t)n_i(t)} - \overline{n_i(t)n_{i+1}(t)}, \tag{59a}$$

$$\frac{d}{dt}\overline{n_i(t)n_{i+1}(t)} = -\overline{n_i(t)n_{i+1}(t)} - \overline{n_{i-1}(t)n_i(t)n_{i+1}(t)} - \overline{n_i(t)n_{i+1}(t)n_{i+2}(t)}, \tag{59b}$$

$$\frac{d}{dt}\overline{n_i(t)n_{i+l}(t)} = -\overline{n_i(t)n_{i+1}(t)n_{i+l}(t)} - \overline{n_i(t)n_{i+l-1}(t)n_{i+l}(t)} - \overline{n_i(t)n_{i+l}(t)n_{i+l+1}(t)} - \overline{n_{i-1}(t)n_i(t)n_{i+l}(t)}, \quad l=2,3,\ldots. \tag{59c}$$

A generalization of Eqs. (59a) and (59b) for strings of k consecutive sites leads again to a hierarchy for the global probabilities $\overline{P}_k(t)$:

$$\frac{d\overline{P}_k(t)}{dt} = -(k-1)\overline{P}_k(t) - 2\overline{P}_{k+1}(t), \quad k=1,2,\ldots,k_{max}. \tag{60}$$

Note that the prefactor of the second term is now 2 due to the additional reactive event between the leftmost particle inside the cluster and a particle at its left-neighbor site. An equation of the form (60) has been obtained in the context of reactant isolation [7] and random sequential adsorption models [16,17]. In these models, the deposition of a dimer on the lattice is equivalent to the desorption of a pair of reactants and empty pairs of sites available for deposition correspond to unreacted pairs of reactants (see Ref. [10]).

The solutions of the hierarchy (60) for a given initial configuration read

$$\overline{P}_k(t) = \exp\{-(k-1)t\} \sum_{j=0}^{k_{max}-k} \frac{\{2\exp(-t)-2\}^j}{j!}\overline{P}_{k+j}(0), \quad k=1,\ldots,k_{max}. \tag{61}$$

(cf. Ref. [18]) from which the mean asymptotic coverage follows straightforwardly

$$c(\infty) = \overline{P}_1(\infty) = \lim_{N\to\infty}\frac{\overline{N_A(\infty)}}{N} = \sum_{j=0}^{k_{max}-1}\frac{(-2)^j}{j!}\overline{P}_{j+1}(0). \tag{62}$$

This result is again in excellent agreement with MC simulations [Fig. 8(a)]. The coarse-grained solution of Eq. (60) is formally obtained by setting $k_{max}=\infty$ and $\overline{P}_j(0)=p^j$. This yields

$$P_1(t) = p\exp[2p\{\exp(-t)-1\}], \tag{63a}$$

$$P_k(t) = p^{k-1}\exp[-(k-1)t]P_1(t), \quad k=2,3,\ldots. \tag{63b}$$

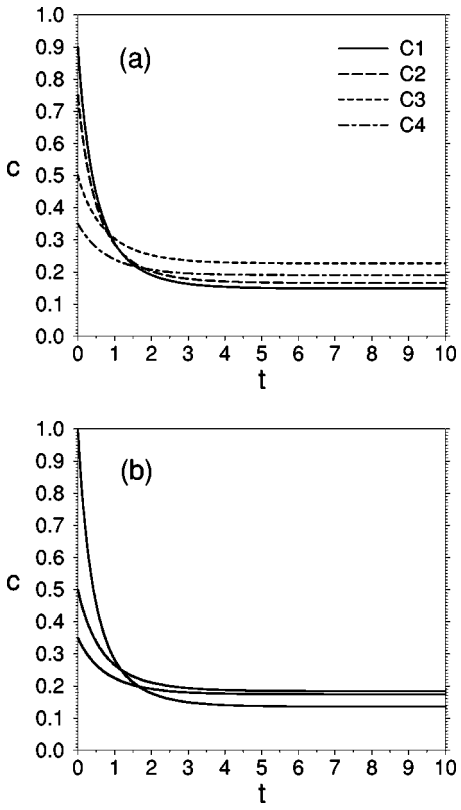

FIG. 8. (a) Mean coverage $c(t)=\overline{P}_1(t)$ for a chain ring of 10^2 sites for the four different initial configurations $C1-C4$ computed from MC simulations over 10^4 realizations [cf. Fig. 2(a)]. Notice, again, the dependence of the asymptotic coverage on the initial conditions. (b) Time evolution of the coarse-grained coverage $c(t)=P_1(t)$ computed from MC simulations over 10^2 realizations for a periodic lattice of 10^4 sites with $p=0.35,0.5$, and 1 (full lattice). In contrast to the CPD case, the behavior of $c(t)$ is no longer monotonic in p for sufficiently large times.

Thus, the corresponding stationary mean coverage takes the form

$$c(\infty) = P_1(\infty) = p\exp(-2p) \tag{64}$$

Note that, contrary to the CPD case, the p-dependence of the asymptotic coverage is no longer monotonic. Thus, as long as $p>0.5$, $c(\infty)$ increases when p is decreased [Fig. 8(b)]. The initial situation of a fully occupied lattice ($p=1$) corresponds in random dimer deposition to an initially empty lattice. In this particular case, a famous combinatorial argument by Flory [19] predicts the value e^{-2} for the asymptotic mean fraction of empty sites (in our picture, occupied sites) at jamming, in accordance with the formula (64).

For the CTD system, it is also possible to derive a truncation hierarchy by introducing fluctuation correlations in Eqs. (59). As in the CPD case, the second-order hierarchy yields a MF steady state, in contradiction with the exact solution of Eq. (60). Once more, the reason for the failure is the non-negligibility of the three-point correlations, some of which can be computed by solving the equation

$$\frac{dP^{(l)}_{j,k}(t)}{dt} = -(j-1)P^{(l)}_{j,k}(t) - (k-1)P^{(l)}_{j,k}(t) - P^{(l-1)}_{j+1,k}(t) - P^{(l)}_{j+1,k}(t) - P^{(l)}_{j,k+1}(t) - P^{(l-1)}_{j,k+1}(t), \quad j,k,l = 1,2,\ldots, \tag{65}$$

which is also found in models for random dimer deposition [20]. As shown in Sec. II D, the correlation functions $P^{(l)}_{j,k}$ can be used to set up explicit equations for the dynamics of vacant sites.

Finally, let us mention that it is possible to rederive the moment equations (59) and the hierarchy (60) from a ME analogous to Eq. (35).

V. SUMMARY AND OUTLOOK

We have developed a one-dimensional CA model that mimics the mesoscopic dynamics of two cooperative desorption reactions. An important advantage of this approach is that one directly sees the effect of a small modification of the MC algorithm on the underlying moment equations. The modeled allows us to derive a hierarchy of linear equations from which the mean particle coverage could be computed for both microscopic and coarse-grained initial conditions. We have seen that a truncation scheme retaining only pair-fluctuation correlations fails to provide the correct behavior of these systems, due to the importance of higher-order fluctuations. However, an alternative truncation based on neglecting the effect of large clusters in the dilute limit yields a smooth expansion of the cluster dynamics in powers of the initial coverage. In the case of the CTD, we have pointed out some analogies with models for dimer deposition.

The CDs studied here are relevant both from a theoretical and from an experimental point of view. Despite their simplicity, they exhibit a complex non-MF behavior characterized by nontrivial memory effects and spontaneous ordering. On the other hand, a large number of physical processes on surfaces involve cooperative desorption of the products [21,22]. In particular, several problems in the context of exciton dynamics in molecular crystals [23,24], recombination of condensed-gas radicals [25], and bond formation in polymers [7] can be mapped into the CDs. A classical example consists of a long polymer chain (methyl vinyl ketone) formed by immobile radical groups that react with nearest neighbors so as to form rings when the chain is heated [7]. Clearly, some groups will be isolated by the reaction dynamics and will remain unreacted. In the CTD model, the unreacted groups can be identified with the A particles and the rings correspond to pairs of vacancies left upon reaction. The quantity of interest, i.e., the fraction of unreacted groups, plays then the role of the lattice coverage.

The effect of incorporating the backward reaction step $S+A \rightarrow A+A$ to the CPD has been studied in Refs. [26,11,12]. In this case, the mixing properties of the system are restored and one attains a MF steady state. It would be desirable to extend the present study to the reversible CTD and also study the influence of an additional random particle input $S \rightarrow A$ on the CDs.

Another possible extension of our work consists of increasing the range of the local interactions by allowing, for instance, interactions with next to nearest neighbors. One expects that the system approaches the MF dynamics as the number of interacting neighbors increases. It is certainly worth to characterize this approach in a more quantitative way.

The dynamics of the one-dimensional CDs changes significantly in the diffusion-limited case [4,27–30]. One can account for the mobility of the particles by introducing additional diffusion terms in the dynamical rule. For the CPD, this has been done in Ref. [31] for initial conditions of the form (27). As expected, diffusion yields an (anomalous) decay into a zero-concentration steady state. The results in Ref. [31] have been compared to an off-lattice solution by ben-Avraham *et al.* [32]. Interestingly, the on-lattice solution displays a slower decay of the coverage for early times due to the finite propagation velocity of a local concentration perturbation on the lattice. A CA approach for the diffusion-limited CDs has been developed by Privman [33]. In the Privman model, all lattice sites are synchronously updated at each time step. An extension of this model for the diffusionless CDs studied above is also worth carrying out.

A natural generalization of our calculations is to study the dynamics of the CDs on Bethe lattices of arbitrary dimension for which results for the cluster dynamics derived heuristically by Majumdar and Privman (see [10]) are available. For the CPD, we expect to obtain results valid for physical lattices as well by extending some expansion methods developed in the framework of dimer deposition [34].

Finally, one would like to extend the boolean CA approach to three-state models accounting for the presence of more than one species and, more generally, to models displaying complex MF behavior like oscillations [35–37] and phase transitions [38,39].

ACKNOWLEDGMENTS

We are indebted to F. Baras, J.P. Boon, H.L. Frisch, A. Provata, and F. Vikas for helpful discussions. This work was supported, in part, by the Training and Mobility of Researchers program of the European Commission and by the Interuniversity Attraction Poles program of the Belgian Federal Government.

APPENDIX A: THE SYMMETRIC CPD

In the symmetric version of the CPD model, a particle at the chosen site *looks* either at the left- or at the right-neighbor site with equal probability and desorbs if the chosen neighbor is occupied. In this case, the dynamical rule reads

$$n_i(t+\Delta t) = n_i(t) - \xi^{(i)}_N(t)\xi_R(t)n_i(t)\{\xi_L(t)n_{i-1}(t) + \{1-\xi_L(t)\}n_{i+1}(t)\}, \quad i=1,\ldots,N. \tag{A1}$$

The additional decision variable $\xi_L(t)$ is equal to one if the left neighbor is chosen and zero otherwise. Clearly, the ad-

ditional choice between left and right may change the global coverage in a realization characterized by a given path $\{\vec{\xi}_N(0), \ldots, \vec{\xi}_N(t)\}$. In contrast, one easily checks that averaging Eq. (A1) leads to the balance equations (20) and (26) valid for the asymmetric system. Clearly, the contributions to the destruction of a cluster by reactive events between two particles inside the cluster are the same in both models. In the asymmetric model, a cluster may be destroyed by the choice of its rightmost particle, which will react with its right-occupied neighbor with probability one. In contrast, this event will only take place with probability $\frac{1}{2}$ in the symmetric model, but there is an additional such contribution due to the reaction of the leftmost particle in the cluster with its left-occupied neighbor. Therefore, both models will lead to the same balance equations for the cluster probabilities $\overline{P}_k(t)$ and $P_k(t)$. This conclusion is supported by comparison of MC simulations performed according to the rules (5) and (A1). A similar argument can be applied to the symmetric CTD.

APPENDIX B: DYNAMICS OF PARTICLE ISLANDS

The definition of a particle cluster introduced in Sec. II C was nonexclusive, meaning that a cluster of a given size could contain smaller clusters. In the following, we will consider a more restrictive definition in which only isolated strings of particles are regarded as distinct clusters. These ''particle islands'' are characterized by the nonvanishing product

$$\{1-n_{i-1}(t)\}\left[\prod_{j=i}^{i+k-1} n_j(t)\right]\{1-n_{i+k}(t)\}, \tag{B1}$$

where k is the size of the island. In a N-site periodic lattice, the total number of islands of size k is given by

$$N_{I,k}(t)=\sum_{i=1}^{N}\{1-n_{i-1}(t)\}\left[\prod_{j=i}^{i+k-1} n_j(t)\right]\{1-n_{i+k}(t)\}, \tag{B2}$$

and the total number of islands is $N_I(t)=\Sigma_{k=1}^{N-1}N_{I,k}(t)$ (the largest island can at most have $N-1$ sites in the ring). With this definition, islands can only be created, never destroyed, even though their size may decrease in time. In order to create a new island at time t, an existing one must be split up by removal of an internal particle (not at the edge of an island). Therefore, the time evolution of $N_I(t)$ will be given by

$$N_I(t+\Delta t)=N_I(t)+\sum_{i=1}^{N}\xi_N^{(i)}(t)n_{i-1}(t)n_i(t)n_{i+1}(t). \tag{B3}$$

In the limit $t\to\infty$, the iteration of this formula yields the total number of particles $N_A(\infty)$ in the steady state

$$\begin{aligned}N_A(\infty)&=N_I(\infty)\\&=N_I(0)\\&\quad+\sum_{j=0}^{\infty}\sum_{i=1}^{N}\xi_N^{(i)}(j\Delta t)n_{i-1}(j\Delta t)n_i(j\Delta t)n_{i+1}(j\Delta t).\end{aligned} \tag{B4}$$

The validity of this formula for the asymptotic coverage induced by a single realization can be easily checked numerically.

Following Sec. II D, we now consider an ensemble of realizations starting from the same initial condition. The probability of finding an island of k consecutive sites can be defined in a similar way to $\overline{P}_k(t)$:

$$\overline{I}_k^{(N)}(t)=\frac{\overline{N}_{I,k}(t)}{N}=\frac{1}{N}\sum_{i=1}^{N}L_k^{(i)}(t), \quad k=1,\ldots,N-1. \tag{B5}$$

with

$$L_k^{(i)}(t)=\{1-n_{i-1}(t)\}\prod_{j=i}^{i+k-1} n_j(t)\{1-n_{i+k}(t)\}. \tag{B6}$$

After some algebra, one obtains

$$\overline{I}_k(t)=\overline{P}_k(t)-2\overline{P}_{k+1}(t)+\overline{P}_{k+2}(t). \tag{B7}$$

Thus, once the solution for the set of $\overline{P}_k(t)$ is known, it is easy to determine the time evolution for the islands. A similar relation is found for coarse-grained initial conditions. In the continuous-time limit, one has

$$\begin{aligned}I_k(t)&=\left\langle\{1-n_{i-1}(t)\}\prod_{j=i}^{i+k-1} n_j(t)\{1-n_{i+k}(t)\}\right\rangle\\&=P_k(t)-2P_{k+1}(t)+P_{k+2}(t)\\&=[1-2p\exp(-t)+p^2\exp(-2t)]P_k(t).\end{aligned} \tag{B8}$$

Note that $I_1(t)$ increases monotonically in time since the number of isolated particles always increases. The situation is less obvious for multiparticle islands (Fig. 9). If the initial coverage is high enough, their number will first be increased due to the breaking of larger islands, however, they will sooner or later be themselves reduced to single-particle islands by the ongoing reactions.

The situation is slightly different in the CTD, since two-particle islands can indeed be destroyed. The evolution of $N_I(t)$ in a single realization is given by

$$\begin{aligned}N_I(t+\Delta t)=N_I(t)&+\sum_{i=1}^{N}\xi_N^{(i)}(t)n_{i-1}(t)n_i(t)n_{i+1}(t)n_{i+2}(t)\\&-\sum_{i=1}^{N}\xi_N^{(i)}(t)\{1-n_{i-1}(t)\}n_i(t)n_{i+1}(t)\\&\times\{1-n_{i+2}(t)\}.\end{aligned} \tag{B9}$$

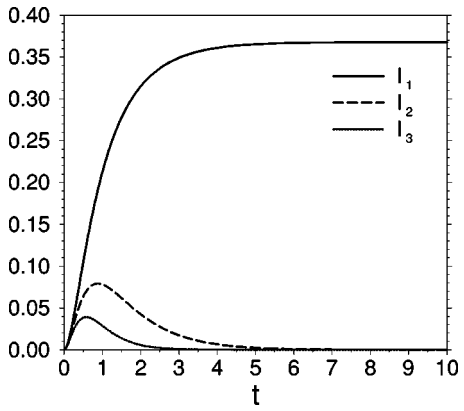

FIG. 9. Time dependence of $I_1(t)$, $I_2(t)$, and $I_3(t)$ according to formula (B8) for an infinite, initially full chain ($p=1$).

The first term describes the creation of a new island by reaction of two internal particles, while the second term stands for the destruction of a two-particle island. The total number of particles in the steady state can be written as

$$N_A(\infty)=N_I(0)+\sum_{j=0}^{\infty}\sum_{i=1}^{N}\xi_N^{(i)}(j\Delta t)n_i(j\Delta t)n_{i+1}(j\Delta t)\times\{n_{i-1}(j\Delta t)+n_{i+2}(j\Delta t)-1\}. \quad \text{(B10)}$$

The dynamics of the islands can be easily determined by using the relations (B7) and (B8), which also hold in this case.

[1] E. V. Albano, Heterog. Chem. Rev. **3**, 389 (1996).
[2] J. P. Boon, D. Dab, R. Kapral, and A. Lawniczak, Phys. Rep. **173**, 55 (1996).
[3] R. Thomas and R. D'Ari, *Biological Feedback* (CRC, Boca Raton, FL, 1990).
[4] T. Liggett, *Interacting Particle Systems* (Springer-Verlag, New York, 1985).
[5] A. S. Mikhailov and A. Y. Loskutov, *Foundations of Synergetics* (Springer, Berlin, 1996).
[6] D. C. Mattis and M. L. Glasser, Rev. Mod. Phys. **70**, 979 (1998).
[7] E. R. Cohen and H. Reiss, J. Chem. Phys. **38**, 680 (1963).
[8] H. Schnoerer, V. Kuzovkov, and A. Blumen, Phys. Rev. Lett. **63**, 805 (1989).
[9] H. Schnoerer, V. Kuzovkov, and A. Blumen, J. Chem. Phys. **92**, 2310 (1990).
[10] S. N. Majumdar and V. Privman, J. Phys. A **26**, L743 (1993).
[11] A. Provata, J. W. Turner, and G. Nicolis, J. Stat. Phys. **70**, 1195 (1993).
[12] S. Prakash and G. Nicolis, J. Stat. Phys. **82**, 297 (1996).
[13] V. M. Kenkre and H. M. Van Horn, Phys. Rev. A **23**, 3200 (1981).
[14] F. Baras, F. Vikas, and G. Nicolis, Phys. Rev. E **60**, 3797 (1999).
[15] E. I. Jury, *Theory and Applications of the z-Transform* (Wiley, New York, 1964).
[16] J. W. Evans, Rev. Mod. Phys. **65**, 1281 (1993).
[17] Y. Fan and J. K. Perkus, Phys. Rev. A **44**, 5099 (1991).
[18] M. C. Bartelt and V. Privman, Int. J. Mod. Phys. B **5**, 2883 (1991).
[19] P. J. Flory, J. Am. Chem. Soc. **61**, 1518 (1939).
[20] J. W. Evans, D. R. Burgess, and D. K. Hoffman, J. Math. Phys. **25**, 3051 (1984).
[21] M. Bowker, *The Basis and Applications of Heterogeneous Catalysis* (Oxford University Press, Oxford, 1998).
[22] V. P. Zdhanov, *Elementary Physicochemical Processes on Surfaces* (Plenum, New York 1991).
[23] V. M. Kenkre, Phys. Rev. B **22**, 2089 (1980).
[24] R. Kopelman, Science **241**, 1620 (1988).
[25] J. L. Jackson and E. W. Montroll, J. Chem. Phys. **28**, 1101 (1958).
[26] A. Sudbury, Ann. Prob. **18**, 581 (1990).
[27] S. Redner and K. Kang, Phys. Rev. A **32**, 435 (1985).
[28] J. L. Spouge, Phys. Rev. Lett. **60**, 871 (1988).
[29] A. A. Lushnikov, Phys. Lett. A **120**, 135 (1987).
[30] F. Family and J. G. Amar, J. Stat. Phys. **65**, 1235 (1991).
[31] E. Abad, H. L. Frisch, and G. Nicolis, J. Stat. Phys. **99**, 1397 (2000).
[32] D. ben-Avraham, M. Burschka, and C. Doering, J. Stat. Phys. **60**, 695 (1990).
[33] V. Privman, Phys. Rev. E **50**, 50 (1994).
[34] J. W. Evans, J. Math. Phys. **25**, 2527 (1984).
[35] F. C. Alcaraz, M. Droz, M. Henkel, and V. Rittenberg, Ann. Phys. (N.Y.) **230**, 250 (1994).
[36] M. Schulz and S. Trimper, J. Phys. A **29**, 6543 (1996).
[37] A. Provata, G. Nicolis, and F. Baras, J. Chem. Phys. **110**, 8361 (1999).
[38] R. M. Ziff, E. Gulari, and Y. Barshad, Phys. Rev. Lett. **56**, 2553 (1986).
[39] J. Marro and R. Dickman, *Nonequilibrium Phase Transitions in Lattice Models* (Cambridge University Press, Cambridge, 1999).